AIAA SciTech Forum
8-12 January 2024, Orlando, FL
AIAA SCITECH 2024 Forum

10.2514/6.2024-0264

In-situ Monitoring with Zero-Bias Deep Neural Network Analysis for Defect Detection and Mitigation in Additively Manufactured Composites

Nicholas Phillips[1], Deepak Kumar[2], Yongxin Liu[3], and Sirish Namilae[4]
Embry-Riddle Aeronautical University, Daytona Beach, FL, 32114, USA

Composite additive manufacturing (AM) is a rapidly growing technology with numerous applications in the aerospace industry. A limiting factor in expanding the application of 3D printed composites is the frequent presence of processing defects. Methods for monitoring and mitigating defects can be helpful in this context. This study focuses on the use of thermography in conjunction with deep learning to identify defects in Onyx, a mixture of chopped carbon fiber and nylon, composite prints. Use of thermography can reveal defect patterns in a printed part before the defects are even visible. The inclusion of a novel zero-bias deep neural network to classify given images can also show real-time monitoring of defects in composite prints as a realizable goal.

I. Introduction

Committee F42 of the American Society of Testing and Materials (ASTM) defines additive manufacturing (AM) as a "general term for technologies that successively join materials to create physical objects specified by 3D model data" [1]. AM, especially of advanced materials such as composites, can be very appealing for many applications owing to its ease of prototyping and ability to achieve high geometrical complexity. Because of these advantages, the aerospace industry is becoming a major consumer of AM technology [2]. Fused deposition modeling (FDM), which has been extensively used to fabricate continuous fiber composites, using thermoplastic matrix materials [3], while direct ink writing (DIW) has been used for short fibers and particulate composites with various matric materials [4].

Despite these advantages, the frequent occurrence of manufacturing defects has limited the application of additively manufactured composites. Defects can occur at any point in the 3D printing process due to any aspect of the printer, printing process, or part geometry [5]. The printing speed, part thickness, line spacing, overhangs, and even the size of a part can contribute to the formation of defects such as warping, void formation, and over-extrusion [6]. The nature of these defects can result in parts that have a fatigue life half as long as the same parts which were produced using traditional subtractive manufacturing methods [7]. Deviations from the optimal range of material and process parameters that affect solidification and curing can cause defects in layer-by-layer construction, such as warping and cracks [5]. Inferior rheological properties lead to instabilities, causing critical geometrical defects, such as inconsistent filaments, stringing, and bulges. This research primarily focuses on the occurrence of warping, void formation, over-extrusion, bed obstructions, and poor bed adhesion in structures made using Onyx, a composite material made from nylon and chopped carbon fibers, produced through fused deposition modeling (FDM).

[1] M.S. Student, Aerospace Engineering, Email: Nicholas.Phillips@my.erau.edu
[2] Ph.D. Student, Aerospace Engineering, Email: Deepak.Kumar@my.erau.edu
[3] Assistant Professor, Mathematics, Email: Youngxin.Liu@my.erau.edu
[4] Professor, Aerospace Engineering, Email: Sirish.Namilae@my.erau.edu

Insitu measurement of parameters that impacted by defect occurrence, such as thermal expansion and cooling patterns, can help understand defect evolution and improve the quality of the printed parts. Thermal imaging cameras are a common method of in-situ data collection and have been used extensively to monitor manufacturing processes [8]. Thermography allows us to detect defects in parts, typically as colder regions, either in the form of a foreign object, the lack of material, or unusual cooling patterns.

Deep neural networks (DNN) are learning algorithms that can identify patterns from a training set of images and use the data from the training images to classify new images based on how closely the new data matches the training data. A few researchers have used various DNN models and approaches for defect detection in additive manufacturing [9-14]. Despite accurate prediction, some of the processes are limited to specific anomaly and data types depending on the training data set. In this study, we used an improved deep neural network (DNN) approach to detect defects. The last dense layer modification of the regular DNN model allowed us to detect unknown anomalies without any prior training of model on any type of abnormal data. If a defect was detected in each image, it would be given its own classification.

II. Experimentation

A. Experiment Setup

The Onyx plates with a layer thickness of 0.2 mm, nozzle temperature of 275°C, and print orientation of 45°/-45°/45°/-45°/45° were fabricated using a Markforged Mark Two printer. A printing pause is applied at the end of each layer. Defects were introduced into the structure by taping a square-shaped copper film onto a print bed. Copper acts as a heat sink to force uneven cooling in the part that leads to defects.

A FLIR A655sc thermal camera was used to capture the thermal data of the additively manufactured plates during the printing process in real-time. This camera has a resolution of 640 × 480 pixels with a measurable temperature range from -40°C to 650°C within +/-2% of the true temperature. The Research-IR software FLIR was used to capture videos and convert them into MATLAB files for post-processing.

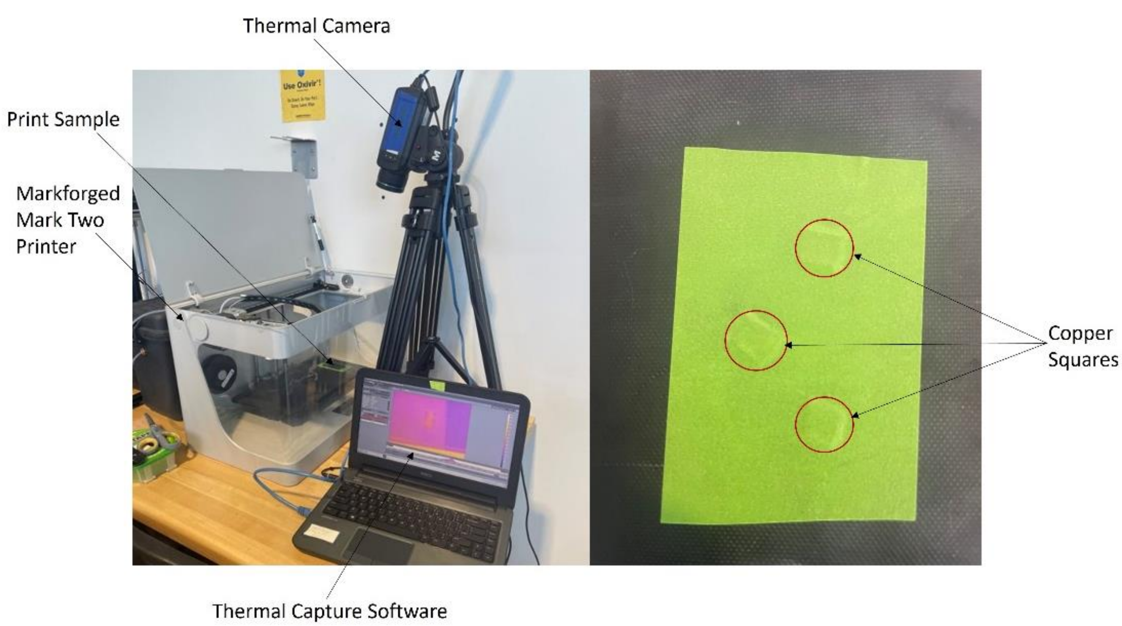

Fig. 1 (left) labeled experiment setup (right) copper layout

B. Zero-Bias Deep Neural Network Setup

Deep neural network models are capable of learning intricate patterns from numerous structured picture datasets and can generate precise predictions based on training data. They are comprised of an input layer, at least one hidden layer, and an output layer, where the output of one layer is the input of another layer. The neurons within a layer have thresholds that trigger the activation of data transference from that neuron to the neurons of the next layer. DNNs can significantly reduce the amount of time required to classify data, such as image classification. However, these traditional methods require high levels of model training, using both non-defected and defective data sets [15-17]. This process limits their capabilities to detect the non-trained image data set and unknown images are forcefully classified into one of the known classes.

In this study, we utilized a novel method for transforming a standard deep neural network model into an abnormality detection model by adding zero bias layers. This method was first developed to detect abnormal fight landings using aviation ADS-B signal data [18]. Recently, we adapted it to additive manufacturing by modifying the input from signal to image to work with image datasets [19]. This approach enables us to detect untrained faults while using only non-defective data sets for training. The last dense layer was modified into two distinct layers—one standard dense layer and the other zero-bias layer. We initially trained the zero-bias DNN model using non-defective datasets and then extracted the feature vector of known data sets from the zero-bias layer. The feature vectors of these known datasets are then utilized to calculate the centroid of each known class and a cutoff distance based on the Mahalanobis Distance (MD) [20] between the class-centered and furthermost feature vectors of each input data sample. If an input's MD from the centroid of each class is more than the cutoff distance for all classes, it is considered an abnormal input. A schematic of the process is shown in Figure 2.

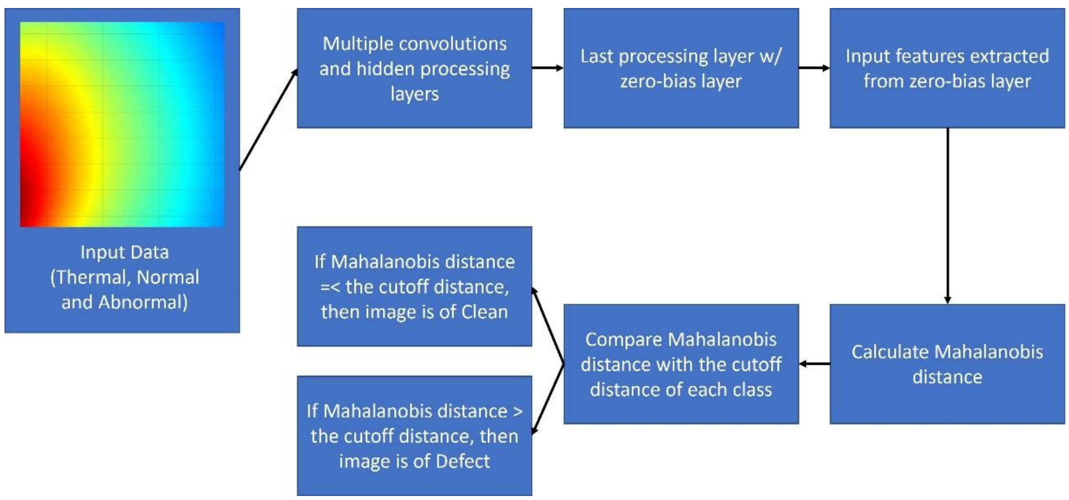

Fig. 2 Flowchart detailing the model training

III. Results

A. In-situ Thermal Characterization of Composite Printing

The Onyx composites were printed in an alternating 45°/-45° layup, which gave the thermal mappings of the layers' distinctive patterns depending on the orientation in which they were printed. The thermal images are captured after each layer is printed. In the 45° layers, which are also odd-numbered layers, the printing starts at the top-left corner and moves toward the bottom-right corner, therefore the thermal image after printing shows higher temperature at the bottom-right corner. In contrast, the -45° printing pattern starts at top-right and ends at bottom-left resulting in higher temperatures at the bottom-left corner in the thermal images. Sample thermal images are shown in Figures 2 (a, b), respectively. It may be noted that the 45° layers displayed a more concentrated hot zone compared to -45° layers which exhibited a flattened and elongated hot zone. This visual matches observations from other studies regarding how ply direction can impact thermal conductivity in a composite [22,23]. In both cases, the cooling patterns were uniform, showing gradual expansion of the gradients without any distortions to the shape, indicating the absence of defects.

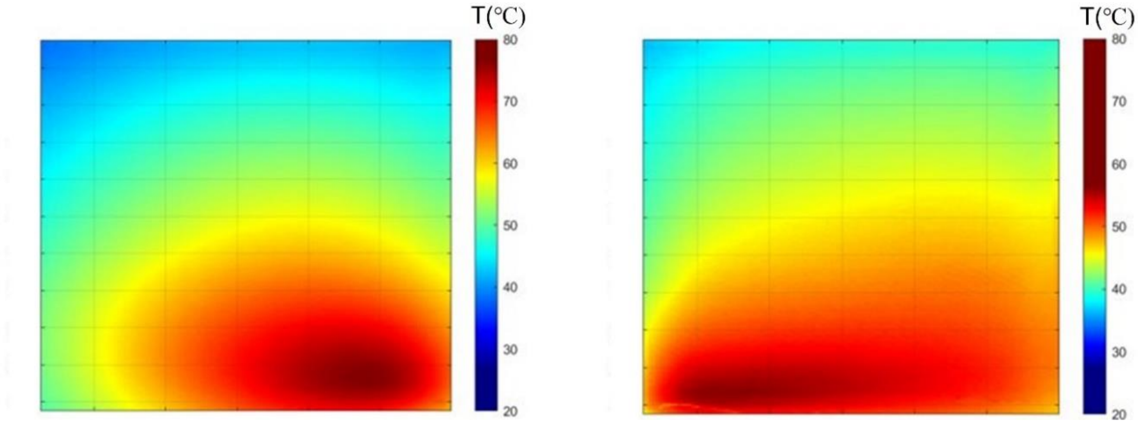

(a) (b)

Fig. 3 Thermal mappings of the first two layers of the clean Onyx print (a) 45º (b) -45º

The defective set of prints displayed similar color gradients to the defect free samples; however, they had clear distortions of colder regions in the shape of the copper squares wrapped around the gradients, as shown in Figure 4. Image subtraction was performed between the defective and non-defective image sets to better highlight the defect locations, which are yellow in the images, as shown in Figure 5.

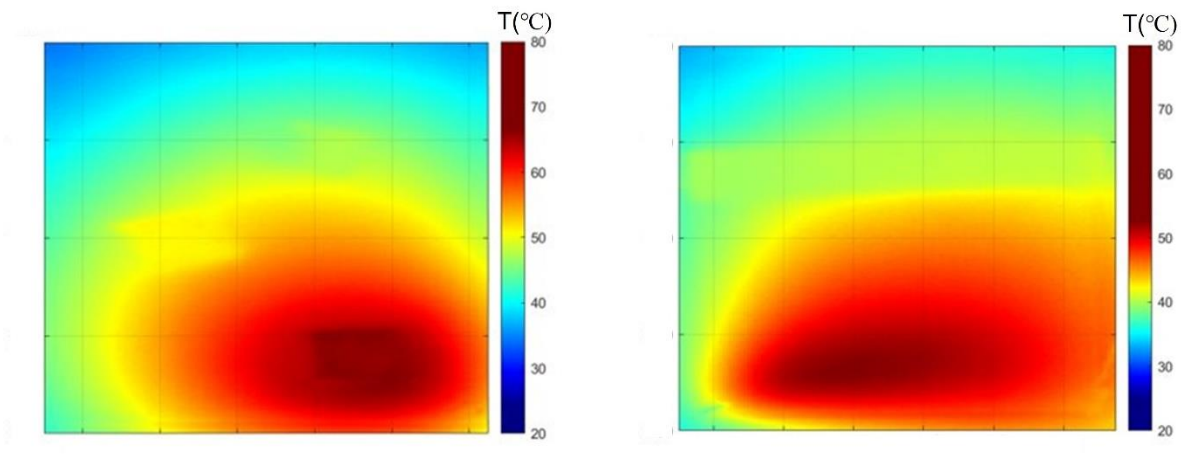

(a) (b)

Fig. 4 Thermal mappings of the first two layers of the defective Onyx print (a) 45º(b) -45º

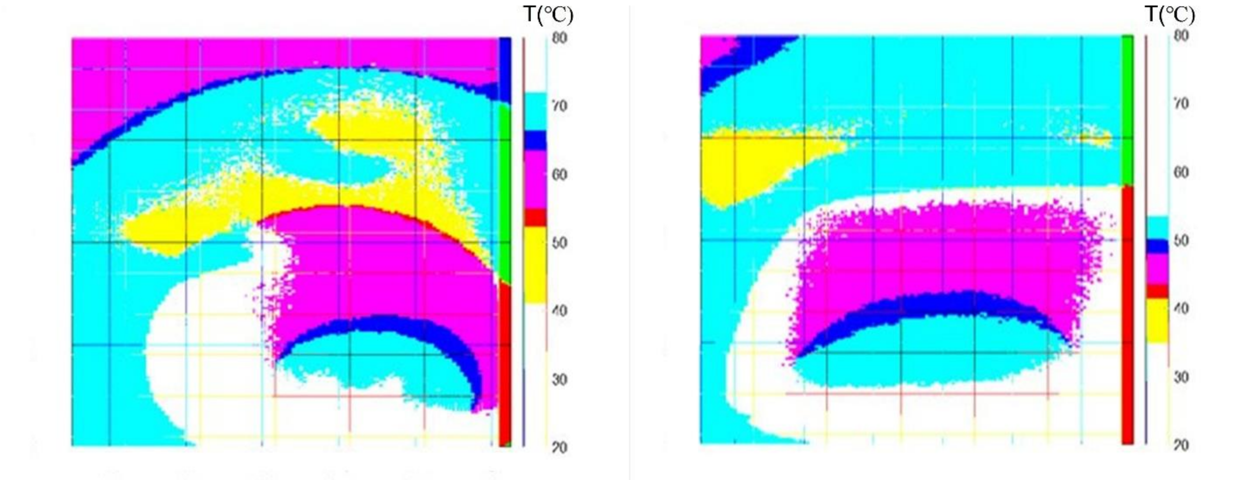

Fig. 5 Subtraction of the images of defects from the images of clean prints

B. Zero bias Deep Neural Network Results

A zero-bias deep neural network framework was utilized to analyze the thermal image data to identify defects. The model was trained using thermal images of samples without defects. 80% of this dataset was used for training and 20% was used for validation. This yielded a training accuracy of 95.28%. Subsequently, the trained model was used to identify defects using an expanded dataset incorporating both normal and abnormal images. The model predictions were recorded as True Positive (TP) if an abnormal image input was correctly predicted as an abnormality, and True Negative (TN) if any normal image was correctly predicted as a normal image. All incorrect predictions are labeled as false negatives (FN) for abnormal images and false positives (FP) for normal images. All the recorded values are plotted in Figure 6 (b), and the overall accuracy was calculated based on the overall prediction rate.

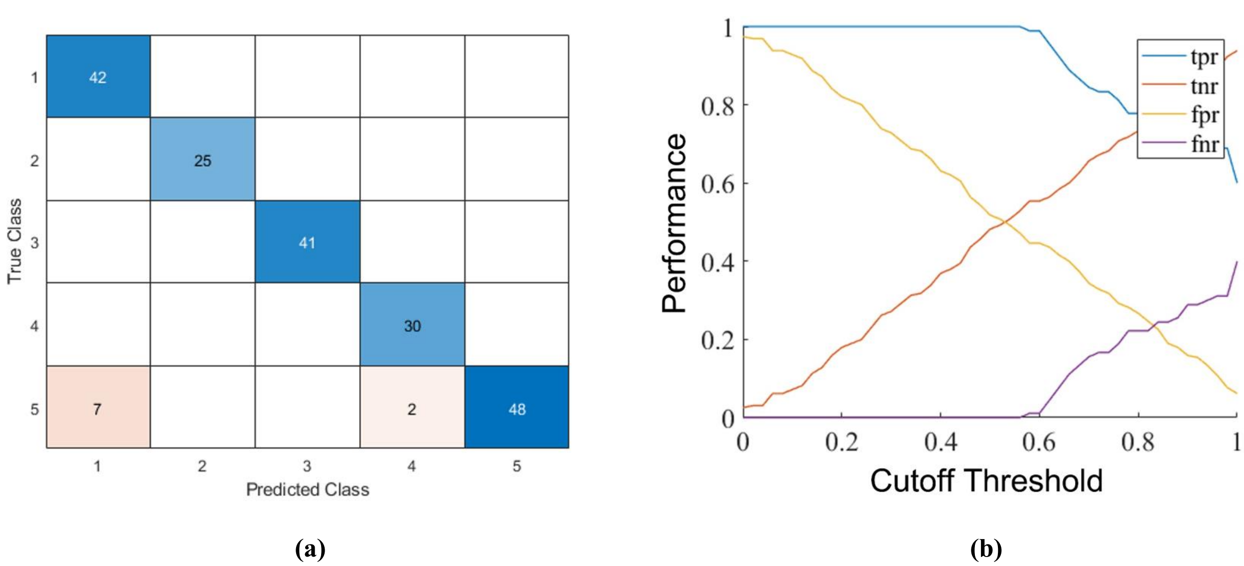

Fig. 6 Zero bias DNN model results of the thermal model (a) Classification of test data sets (b) Abnormality detection performance

We used a graphical approach to visualize known and unknown dataset variations in the latent decision space. Because the zero-bias layer acts as a similarity-matching layer, we can consider its weights as a class fingerprint for an input image. The dimension of each extract feature vector from the zero bias layer is reduced by using a nonlinear dimension reduction method t-distributed stochastic neighbor embedding (t-SNE) [21] and plotted using a Voronoi diagram. The class fingerprint extracted from the zero-bias layer is represented by a triangle, as shown in Figure 7. In Figure 8, each dot filled with color represents a known data (normal) input and each empty dot represents an abnormal image input, which in the case of this research is a defect. Inset in Figure 7 shows a zoomed-in of what appears to be a single data point from Figures 7 and 8 but reveals that these points are clusters of smaller points.

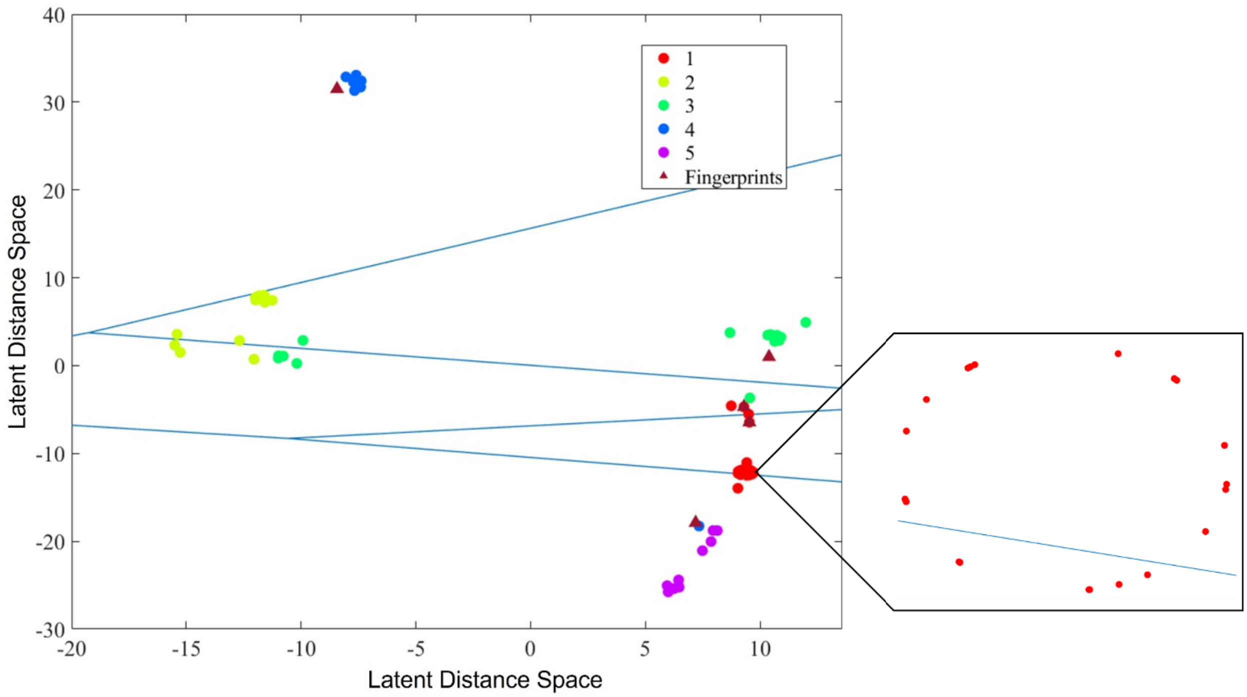

Fig. 7 Voronoi diagram of the thermal test without defects (left) and zoom in on a "point" (right)

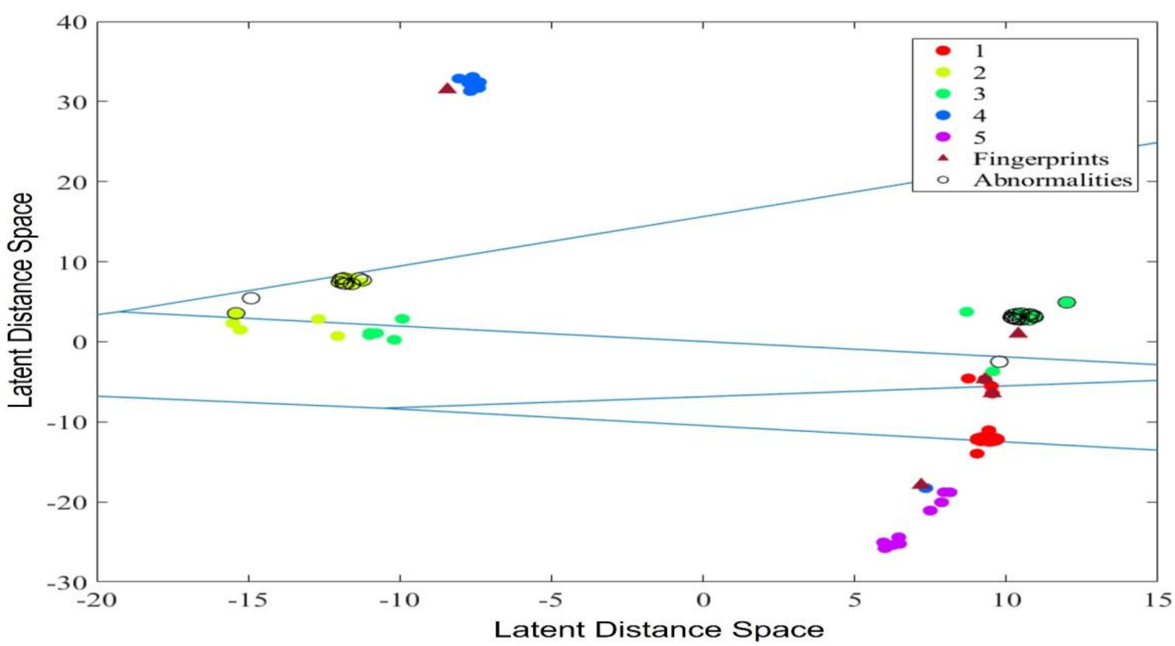

Fig. 8 Voronoi diagram of the thermal test with defects

IV. Discussion

In this study, a unique approach based on a zero-bias deep neural network was used to detect defects in additively manufactured composites. A regular DNN model was modified by adding a new zero-bias layer after the regular dense layer, which was later used to extract the feature vector of each input sample. The overall anomaly detection theory was based on the condition that the feature vector of the defective sample had a higher MD than the without defect sample from all known class centers. We targeted these differences between the feature vectors of the normal and abnormal samples and converted a regular DNN model into an abnormality detection model. This explainable approach overcomes some of the limitations of the currently available methods for defect detection, such as the lack of information about the hidden layer calculation for defected and undetected sample input. An explainable DNN model is more acceptable in terms of trustworthiness and accuracy for real applications. Another limitation of most available methods is that they must be trained on all possible abnormal and normal sample inputs prior to detecting anomalies, which increases the requirement of training data, training time, and computational power. However, the zero-bias approach used in this study is independent of anomaly types, shape, and location, and only needs to be trained on normal datasets. This characteristic of the zero-bias approach makes it more suitable for multiple future modifications and applications such as real-time process monitoring for defect detection and mitigation. The approach developed in this study is material independent and can be easily adapted to different material combinations using FDM, as well as other similar additive manufacturing processes.

V. Conclusion

In this study, in-situ thermal imaging was used to observe and analyze defect formation in composite additive manufacturing during the printing process. The thermal data displayed notable differences in cooling patterns between clean and defective prints. The data collected from the in-situ observations was further analyzed using a deep neural network to classify images and detect abnormalities. The DNN was modified to include a zero-bias layer which ensured that generic defective images could be identified without explicitly training on defective images. This study was able to produce a model training accuracy of 95.28%, which was adequate to identify anomalies during the additive manufacturing process.

Acknowledgments

We would like to thank Dr. Jeff Brown for providing the thermal camera used for the research and insightful feedback regarding the analysis of the thermal data. This research was supported by National Science Foundation (NSF) Advanced Manufacturing Grant # 2001038.

VI. References

[1] ISO/ASTM 52900:2021(en), 'Additive manufacturing — General principles — Fundamentals and vocabulary', International Organization for Standardization, 2021.

[2] Blakey-Milner, B., Gradl, P., Snedden, G., Brooks, M., Pitot, J., Lopez, E., Leary, M., Berto, F., and du Plessis, A., "Metal additive manufacturing in aerospace: A review" Materials & Design, Volume 209, 2021, https://doi.org/10.1016/j.matdes.2021.110008.

[3] Penumakala, P. K., Santo, J., and Thomas, A., 'A critical review on the fused deposition modeling of thermoplastic polymer composites', Composites Part B: Engineering, vol. 201. 2020. doi: 10.1016/j.compositesb.2020.108336.

[4] Franchin, G., Wahl, L., and Colombo, P., 'Direct ink writing of ceramic matrix composite structures', Journal of the American Ceramic Society, vol. 100, no. 10, 2017, doi: 10.1111/jace.15045.

[5] Tamir, T. S., Xiong, G., Shen, Z., Leng, J., Fang, Q., Yang, Y., Jiang, J., Lodhi, E., and Wang, F., "3D printing in materials manufacturing industry: A realm of Industry 4.0", Heliyon, Volume 9, Issue 9, 2023, https://doi.org/10.1016/j.heliyon.2023.e19689.

[6] Englert, L., Czink, S., Dietrich, S., and Schulze, V., "How defects depend on geometry and scanning strategy in additively manufactured AlSi10Mg", Journal of Materials Processing Technology, Volume 299, 2022, https://doi.org/10.1016/j.jmatprotec.2021.117331

[7] Mostafaei, A., Zhao, C., He, Y., Ghiaasiaan, S. R., Shao, B. S. S., Shamsaei, N., Wu, Z., Kouraytem, N., Sun, T., Pauza, J., Gordon, J. V., Webler, B., Parab, N. D., Asherloo, M., Guo, Q., Chen, L., and Rollett, A. D., "Defects and anomalies in powder bed fusion metal additive manufacturing", Current Opinion in Solid State and Materials Science, Volume 26, Issue 2, 2022, https://doi.org/10.1016/j.cossms.2021.100974

[8] FLIR, "An Overview of Thermography for Mechanical Applications", 2018, https://www.flir.com/support-center/training/thermography-training/webinars/an-overview-ofthermography-for-mechanical-applications/

[9] Caggiano, A., Zhang, J., Alfieri, V., Caiazzo, F., Gao, R. and Teti, R., (2019), "Machine learning-based image processing for on-line defect recognition in additive manufacturing", CIRP Annals, Vol. 68, doi: 10.1016/j.cirp.2019.03.021.

[10] Grasso, M., Demir, A.G., Previtali, B. and Colosimo, B.M., (2018), "In situ monitoring of selective laser melting of zinc powder via infrared imaging of the process plume", Robot ComputIntegrManuf, Vol. 49, doi: 10.1016/j.rcim.2017.07.001.

[11] Delli, U. and Chang, S., (2018), "Automated process monitoring in 3D printing using supervised machine learning", doi: 10.1016/j.promfg.2018.07.111

[12] Paraskevoudis, K., Karayannis, P. and Koumoulos, E.P., (2020), "Real-time 3d printing remote defect detection (stringing) with computer vision and artificial intelligence", Processes, Vol. 8 No. 11, doi: 10.3390/pr8111464.

[13] Zhang, Y., Hong, G.S., Ye, D., Zhu, K. and Fuh, J.Y.H., (2018), "Extraction and evaluation of melt pool, plume and spatter information for powder-bed fusion AM process monitoring", Materials & Design, Vol. 156, doi: 10.1016/j. Matdes.2018.07.002

[14] Scime, L. and Beuth, J., (2019), "Using machine learning to identify in-situ melt Pool signatures indicative of flaw formation in a laser powder bed fusion additive manufacturing process", Additive Manufacturing, Vol. 25, doi: 10.1016/j. Addma.2018.11.010

[15] A. Caggiano, J. Zhang, V. Alfieri, F. Caiazzo, R. Gao, and R. Teti, 'Machine learning-based image processing for on-line defect recognition in additive manufacturing', CIRP Annals, vol. 68, no. 1, 2019, doi: 10.1016/j.cirp.2019.03.021

[16] Chen, Z., Yeo, C. K., Lee, B. S., and Lau, C. T. 'Autoencoder-based network anomaly detection', in Wireless Telecommunications Symposium, 2018. doi: 10.1109/WTS.2018.8363930.

[17] Chow, J. K., Su, Z., Wu, J., Tan, P. S., Mao, X., and Wang, Y. H., 'Anomaly detection of defects on concrete structures with the convolutional autoencoder', Advanced Engineering Informatics, vol. 45, 2020, doi: 10.1016/j.aei.2020.101105.

[18] Liu, Y., Wang, J., Li, J., Niu, S., Wu, L., and Song, H. 'Zero-Bias Deep-Learning-Enabled Quickest Abnormal Event Detection in IoT', IEEE Internet Things J, vol. 9, no. 13, 2022, doi: 10.1109/JIOT.2021.3126819.

[19] Kumar, Deepak, Yongxin Liu, Houbing Song, and Sirish Namilae. "Explainable deep neural network for in-plain defect detection during additive manufacturing." Rapid Prototyping Journal (2023)

[20] De Maesschalck, R., Jouan-Rimbaud, D. and Massart, D.L.(2000), "The Mahalanobis distance", Chemometrics and Intelligent Laboratory Systems, Vol. 50 No. 1, doi: 10.1016/S0169-7439(99)00047-7.

[21] Van Der Maaten, L. and Hinton, G., 'Visualizing data using t-SNE', Journal of Machine Learning Research, vol. 9, 2008.

[22] Yu, H., Heider, D., and Advani, A., "Role of in-plane stacking sequence on transverse effective thermal conductivity of unidirectional composite laminates", *International Journal of Heat and Mass Transfer*, Volume 85, 2015, Pages 897-903, https://doi.org/10.1016/j.ijheatmasstransfer.2015.02.003.

[23] Ali, M. Sobolciak, P. Krupa, I. and Abdala, A., "Impact of the Processing-Induced Orientation of Hexagonal Boron Nitride and Graphite on the Thermal Conductivity of Polyethylene Composites", *Polymers,* 2023; 15(16):3426. https://doi.org/10.3390/polym15163426